Continuous Bracing Requirements for Constrained-Axis Torsional Buckling

MARK D. DENAVIT, WILLIAM P. JACOBS V, and TODD A. HELWIG

ABSTRACT

The design of floor and roof framing members is typically controlled by flexural demands; however, if a member serves as a chord or collector, it can also be subjected to significant axial compression. Continuous restraint provided by the floor or roof diaphragm is commonly assumed in design to provide adequate bracing of connected wide-flange members against minor-axis flexural buckling; however, these members are still susceptible to major-axis flexural buckling and potentially to torsional buckling about a constrained axis located at the top flange. In addition to the lateral restraint, floor and roof decking systems can also provide continuous torsional restraint through their flexural stiffness and strength. This restraint can be used to increase the calculated constrained-axis torsional buckling strength or inhibit the mode altogether. In this paper, the specific case of a wide-flange steel beam-column with both lateral and torsional restraint located at the top flange is investigated, and torsional bracing requirements are derived. The focus of the study is on continuous torsional bracing and its effect on the constrained-axis torsional buckling mode. The requirements are illustrated through a design example, and a parametric study is performed examining typical floor and roof decking system configurations, identifying cases where improved design efficiency can be achieved.

Keywords: Axial strength, constrained-axis torsional buckling, stability, wide-flange shapes.

INTRODUCTION

In building structures, floor or roof framing members that serve as chords or collectors can accumulate significant axial load as they transfer loads from the diaphragm to the vertical elements of the lateral-force-resisting system. The strength of these members in compression can be governed by a number of different buckling modes. Figure 1 depicts the potential member buckling modes that might control the axial strength. Although designers are familiar with the flexural buckling modes for wide-flange columns as shown in Figures 1(a) and 1(b), these members are also susceptible to torsional buckling when the bracing does not prevent twist and the unbraced length for torsional buckling is larger than the unbraced length for minor-axis flexural buckling. If the lateral bracing is located at the shear center (which coincides with the centroid for wide-flange sections), the torsional buckling mode as depicted in Figure 1(c) is possible. The strength for torsional buckling about the shear center can be predicted using the expressions in AISC *Specification* Section E4 (AISC, 2016). However, if the lateral bracing is offset from the centroid, the member can fail by constrained-axis torsional buckling as depicted in Figure 1(d) (for a case where the lateral bracing is located at the top of the top flange of the member), and the expressions provided in the Commentary on Section E4 are necessary as outlined in the next section of this paper.

When wide-flange beams are laterally restrained by a decking system, the limit states of minor-axis flexural buckling and torsional buckling [twisting about the shear center as shown in Figure 1(c)] are not applicable. As stated in AISC *Seismic Design Manual* (AISC, 2018), Table 8-1, this restraint occurs for bare steel deck (either steel roof deck or composite steel deck prior to placement of the concrete) when the ribs of the deck are perpendicular to the beam and for composite slabs (i.e., composite steel deck with concrete fill) in any orientation. The axial strength of the member for these cases is calculated from the limit states of major-axis flexural buckling and constrained-axis torsional buckling. Bare steel deck with ribs parallel to the beam is commonly assumed to provide inadequate lateral restraint and thus is not addressed in this paper.

The discussion thus far has focused on cases in which the decking system only restrains lateral movement. However, decking systems also provide torsional restraint to the beam. While it is conservative to neglect this restraint, in many cases the restraint is sufficient to brace the beam against constrained-axis torsional buckling or otherwise significantly increase the calculated strength. In this paper, bracing requirements for constrained-axis torsional buckling are developed. A detailed example is presented that illustrates

Mark D. Denavit, Assistant Professor, University of Tennessee, Knoxville, Tenn. Email: mdenavit@utk.edu (corresponding)

William P. Jacobs V, Principal, Stanley D. Lindsey and Associates, Ltd., Atlanta, Ga. Email: wjacobs@sdlal.com

Todd A. Helwig, Professor, J. Neils Thompson Teaching Fellow in Civil Engineering, University of Texas at Austin, Austin, Tex. Email: thelwig@mail.utexas.edu

Paper No. 2019-07

the use of these requirements for common applications such as the design of collector beams or other members subjected to large axial forces. Finally, the results of a broad parametric study are presented with observations that highlight configurations where the benefits of the torsional restraint are most effective.

Although the "beams" in the flooring or roofing system that are discussed in this paper are actually "beam-columns" due to the combined axial force and bending moment, the term "beams" is used throughout the paper for convenience. The focus of the bracing requirements in the paper is the stiffness and strength requirements necessary to control the constrained-axis torsional buckling mode from the axial force component.

CONSTRAINED-AXIS TORSIONAL BUCKLING STRENGTH

The design of members for compression is governed by the provisions of Chapter E in the AISC *Specification* (AISC, 2016). The nominal axial compressive strength in the elastic and inelastic range is determined from the column curve expressions given in Section E3:

$$P_n = F_{cr} A_g \tag{1}$$

$$F_{cr} = \begin{cases} 0.658^{\left(F_y/F_e\right)} F_y & \text{when } F_y/F_e \le 2.25 \\ 0.877 F_e & \text{when } F_y/F_e > 2.25 \end{cases} \tag{2}$$

where

A_g = gross cross-sectional area, in.^{2}
F_{cr} = critical stress, ksi
F_e = elastic buckling stress, ksi
F_y = yield stress, ksi
P_n = nominal compressive strength, kips

If a section has slender elements, the provisions of Section E7 can be used to determine the effective area, A_e, that is used in place of A_g in Equation 1. The methodology for accounting for slender elements is covered in more detail later in this section as well as in the example problem that is presented in this paper.

For constrained-axis torsional buckling with bracing offset along the minor axis, as shown in Figure 2, the elastic buckling stress is given by AISC *Specification* (2016) Commentary Equation C-E4-1, shown here as Equation 3. The fundamental equation for this mode was developed by Timoshenko and Gere (1961). The expression presented in the Commentary is slightly modified as recommended by Errera and Apparao (1976) and Helwig and Yura (1999) to account for practical limitations that often occur in practice.

$$F_e = \omega \left[\frac{\pi^2 E I_y}{L_{cz}^2} \left(\frac{h_o^2}{4} + a^2 \right) + GJ \right] \frac{1}{A_g r_o^2} \tag{3a}$$

$$r_o^2 = r_x^2 + r_y^2 + a^2 \tag{3b}$$

where

E = modulus of elasticity of steel = 29,000 ksi
G = shear modulus of steel = 11,200 ksi
I_y = minor-axis moment of inertia, in.^{4}
J = torsional constant, in.^{4}
L_{cz} = effective torsional length, in.
a = distance from centroid to brace point, in.
h_o = distance between flange centroids, in.
r_x = major-axis radius of gyration, in.
r_y = minor-axis radius of gyration, in.
ω = finite brace stiffness factor = 0.9

Although wide-flange sections with slender elements are not typically used as columns, many beam-type sections are slender for axial compression. As a result, a wide-flange section that might be used in a flooring system may possess slender elements for compression. In such a case, the interaction of constrained-axis torsional buckling and local buckling should be accounted for in accordance with AISC *Specification* Section E7. The effective area, A_e, is computed as a function of the critical buckling stress, F_{cr}. For the case

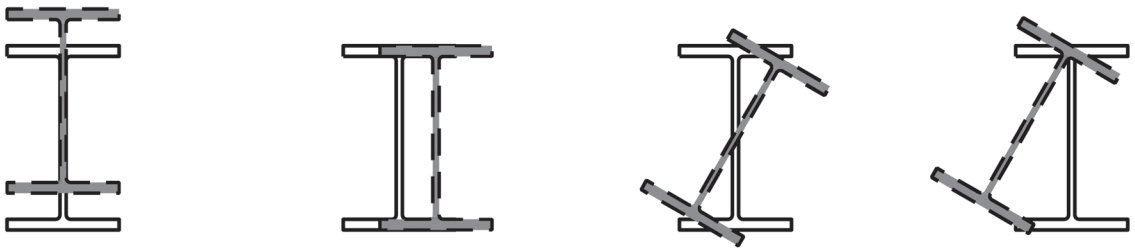

Major-axis flexural buckling (a) | *Minor-axis flexural buckling (b)* | *Torsional buckling (c)* | *Constrained-axis torsional buckling (d)*

Fig. 1. Buckling modes.

of wide-flange steel members, A_e is computed as shown in Equation 4, where the effective widths of the flange and web are computed using Equations 5 and 6, respectively.

$$A_e = A_g - 4(b_f/2 - b_e)t_f - (h - h_e)t_w \tag{4}$$

$$b_e = \begin{cases} b_f/2 & \text{when } \lambda_f \le \lambda_{rf}\sqrt{F_y/F_{cr}} \\ \left(1 - 0.33\dfrac{\lambda_{rf}}{\lambda_f}\sqrt{\dfrac{F_y}{F_{cr}}}\right)1.49\dfrac{\lambda_{rf}}{\lambda_f}\sqrt{\dfrac{F_y}{F_{cr}}}\dfrac{b_f}{2} & \text{when } \lambda_f > \lambda_{rf}\sqrt{F_y/F_{cr}} \end{cases} \tag{5a}$$

$$\lambda_{rf} = 0.56\sqrt{\frac{E}{F_y}} \tag{5b}$$

$$\lambda_f = \frac{b_f}{2t_f} \tag{5c}$$

$$h_e = \begin{cases} h & \text{when } \lambda_w \le \lambda_{rw}\sqrt{F_y/F_{cr}} \\ \left(1 - 0.24\dfrac{\lambda_{rw}}{\lambda_w}\sqrt{\dfrac{F_y}{F_{cr}}}\right)1.31\dfrac{\lambda_{rw}}{\lambda_w}\sqrt{\dfrac{F_y}{F_{cr}}}h & \text{when } \lambda_w > \lambda_{rw}\sqrt{F_y/F_{cr}} \end{cases} \tag{6a}$$

$$\lambda_{rw} = 1.49\sqrt{\frac{E}{F_y}} \tag{6b}$$

$$\lambda_w = \frac{h}{t_w} \tag{6c}$$

Further discussion of constrained-axis torsional buckling strength including design tables and example calculations are provided in Liu et al. (2013). AISC *Design Guide* 25 (Kaehler et al., 2011) describes recommendations for computing the constrained-axis torsional buckling strength for singly symmetric and tapered members.

BRACING REQUIREMENTS

Effective stability bracing must possess adequate stiffness and strength. Brace stiffness and strength requirements to control torsional buckling and constrained-axis torsional buckling were developed by Helwig and Yura (1999), based upon the results of a parametric finite element study. For the case of discrete bracing and considering inelastic buckling, the required torsional brace stiffness is given by Equation 7.

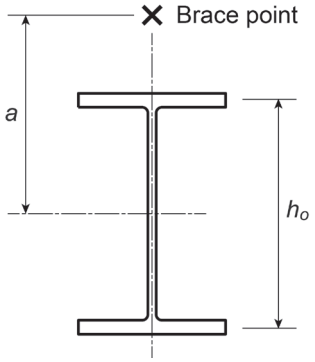

Fig. 2. Bracing offset along minor axis.

$$\beta_T = A\frac{\left\{P_u r_o^2 - P_{ny}^*\left[(h_o^2/4) + a^2\right]\right\}^2}{(n_b 4\tau EI_y/L)\left[(h_o^2/4) + a^2\right]} \tag{7a}$$

$$A = 4 - \frac{2a}{h_o} \ge 2.0 \tag{7b}$$

$$P_{ny}^* = 0.877\tau\frac{\pi^2 EI_y}{L^2} \tag{7c}$$

where

L = beam span, in.
P_u = required axial compressive strength, kips
n_b = number of intermediate braces
β_T = required brace stiffness
τ = stiffness reduction factor

The stiffness reduction factor, τ, is applied to account for the reduced stiffness and strength due to inelasticity and local buckling and has been modified from the original presentation given in Helwig and Yura (1999) to reflect the provisions in the current AISC *Specification* (2016), as shown in Equation 8.

$$\tau = \begin{cases} -2.724(P_u/P_y)\ln(P_u/xP_y) & \text{when} \quad P_u/xP_y > 0.39 \\ x & \text{when} \quad P_u/xP_y \le 0.39 \end{cases} \tag{8a}$$

$$x = \frac{A_e\big|_{F_{cr}=P_u/A_e}}{A_g} \tag{8b}$$

where

P_y = axial yield strength, kips
$= F_y A_g$
x = ratio of the effective area (calculated iteratively for a critical stress equal to the required axial strength divided by the effective area) to the gross area

Alternatively, for previous versions of the AISC *Specification* (e.g., 2010) where the strength of members with slender elements was calculated using the net reduction factor, Q, the stiffness reduction factor should be taken as Equation 9, where Q is calculated at the required axial strength.

$$\tau = \begin{cases} -2.724(P_u/QP_y)\ln(P_u/QP_y) & \textit{when} \quad P_u/QP_y > 0.39 \\ 1.0 & \textit{when} \quad P_u/QP_y \le 0.39 \end{cases} \tag{9}$$

The required brace stiffness (Equation 7a) is modified for the case of a member braced continuously at the top flange by (1) substituting in the location of the brace at the centroid of the top flange ($a = h_o/2$) and (2) converting from discrete to continuous bracing by setting the term n_b/L equal to unity (note that after this change, β_T is expressed as the torsional stiffness per unit length). Additionally, a resistance factor of $\phi = 0.75$ is applied according to AISC *Specification* Appendix 6 (2016). The resulting expression is given by Equation 10.

$$\beta_T = \frac{1.5}{\phi}\frac{\left(P_u r_o^2 - P_{ny}^* h_o^2/2\right)^2}{\tau E I_y h_o^2} \tag{10}$$

There are a number of factors that can affect the total brace stiffness, including the stiffness of the decking system as well as other stiffness components such as cross-sectional distortion due to flexibility in the beam web and connection stiffness between the decking system and beam. In the derivation presented herein, the total brace stiffness is based on the stiffness of the decking system acting in series with the distortional stiffness of the beam web, β_{sec}, given in Equation 11 (AISC *Specification* Equation A-6-13). In this paper, the connection between the decking system and the beam is assumed to be rigid. Accordingly, the required stiffness of the decking system, β_{Tb}, is given by Equation 12 (AISC *Specification* Equation A-6-10). Note that if the web distortional stiffness is less than or equal to the required total brace stiffness ($\beta_{sec} \le \beta_T$), then Equation 12 is negative and the required total brace stiffness cannot be achieved regardless of the stiffness provided by the decking system.

$$\beta_{\text{sec}} = \frac{3.3Et_w^3}{12h_0} \tag{11}$$

$$\beta_{Tb} = \frac{\beta_T}{\left(1 - \frac{\beta_T}{\beta_{\text{sec}}}\right)} \tag{12}$$

where β_{Tb} = required stiffness of the decking system.

As noted by Helwig and Yura (1999), the required brace stiffness limits the twist of the beam due to the applied loading to a value equal to the initial twist imperfection. Thus, the resulting brace strength requirement is the product of the required brace stiffness, β_T, and the initial twist imperfection θ_0, as shown in Equation 13. The assumed initial twist imperfection is based on a configuration where one flange is straight and the other flange has a lateral initial out-of-straightness with maximum lateral imperfection of $L/500$. This results in an assumed initial twist imperfection given by Equation 14.

$$M_{br} = \beta_T \theta_0 \tag{13}$$

$$\theta_0 = \frac{L}{500h_o} \tag{14}$$

Often, the stiffness provided by the decking system is more than sufficient to brace the beam, leaving strength as the limiting brace requirement. In these cases, the required moment strength can be reduced as a function of the ratio of required to provided stiffness as given by Equation 15 based on Equation C-A-6-2 from the AISC *Specification* Commentary (2016). The total provided stiffness, β_{prov}, is computed using an expression for springs in series given in Equation 16, where the stiffness provided by the deck, $\beta_{prov\text{-}b}$, is combined with the web distortional stiffness, β_{sec}.

$$M_{br} = \frac{\beta_T \theta_o}{\left(2 - \beta_T/\beta_{prov}\right)} \tag{15}$$

$$\frac{1}{\beta_{prov}} = \frac{1}{\beta_{prov-b}} + \frac{1}{\beta_{sec}} \tag{16}$$

The example outlined in the following section illustrates the use of these bracing provisions for details commonly found in practice.

DESIGN EXAMPLE

Given:

Consider a 24-ft-long W18×35 ASTM A992 beam supporting a composite slab that has a total depth of 6 in., normal weight concrete ($f_c' = 3$ ksi), and 3-in. deep, 20-ga. composite steel deck. The deck spans perpendicular to the beams that are spaced at 10 ft. Steel headed stud anchors of ASTM A108 material with a diameter of ¾ in. are provided at a spacing, s, of 1 ft. The beam is assumed to be simply supported with twist restrained but warping deformations permitted at the ends.

Solution:

The problem is worked in multiple steps to illustrate the various modes as well as the contributions of the bracing. Baseline calculations are first carried out to understand the flexural and torsional modes, neglecting the contributions of the composite slab. It should be understood that although the lateral stiffness of the composite slab is neglected in the calculation of the minor-axis flexural buckling mode, the lateral stiffness is required for the constrained-axis torsional buckling mode to occur. The shear stiffness of most typical decking systems (bare composite steel or roof deck with ribs perpendicular to the braced member or composite slabs in any orientation) is most often much larger than necessary to provide adequate lateral bracing.

Baseline Calculations

Determine the nominal strength for the limit state of constrained-axis torsional buckling neglecting the torsional stiffness provided by the decking system.

From AISC *Manual* Table 2-4, the beam yield stress is:

$F_y = 50$ ksi

From AISC *Manual* Table 1-1 (AISC, 2017a), the relevant section properties for the beam are:

$A_g = 10.3$ in.^{2}	$I_x = 510$ in.^{4}	$I_y = 15.3$ in.^{4}	$J = 0.506$ in.^{4}
$b_f = 6.00$ in.	$d = 17.7$ in.	$t_w = 0.300$ in.	$t_f = 0.425$ in.
$r_x = 7.04$ in.	$r_y = 1.22$ in.	$b_f/2t_f = 7.06$	$h/t_w = 53.5$
$h_o = 17.3$ in.	$h = 16.1$ in.	$k_1 = 0.75$ in.	

The effective length of the beam is taken as the full span because twist is restrained but warping deformations are permitted at the ends of the beam.

$$\begin{aligned} L_{cz} &= L \\ &= (24 \text{ ft})(12 \text{ in./ft}) \\ &= 288 \text{ in.} \end{aligned}$$

To determine the elastic buckling stress, F_e, using Equation 3a, first determine a and r_o^2.

$$\begin{aligned} a &= \frac{h_o}{2} \\ &= \frac{17.3 \text{ in.}}{2} \\ &= 8.65 \text{ in.} \end{aligned} \tag{3b}$$

$$\begin{aligned} r_o^2 &= r_x^2 + r_y^2 + a^2 \\ &= (7.04 \text{ in.})^2 + (1.22 \text{ in.})^2 + (8.65 \text{ in.})^2 \\ &= 126 \text{ in.}^2 \end{aligned}$$

$$F_e = \omega \left[\frac{\pi^2 E I_y}{L_{cz}^2} \left(\frac{h_o^2}{4} + a^2 \right) + GJ \right] \frac{1}{A_g r_o^2} \tag{3a}$$

$$= 0.90 \left[\frac{\pi^2 (29{,}000 \text{ ksi})(15.3 \text{ in.}^4)}{(288 \text{ in.})^2} \left(\frac{(17.3 \text{ in.})^2}{4} + (8.65 \text{ in.})^2 \right) + (11{,}200 \text{ ksi})(0.506 \text{ in.}^4) \right] \frac{1}{(10.3 \text{ in.}^2)(126 \text{ in.}^2)}$$

$$= 9.42 \text{ ksi}$$

Compute the critical stress, F_{cr}, using Equation 2.

$$\begin{aligned} \frac{F_y}{F_e} &= \frac{50 \text{ ksi}}{9.42 \text{ ksi}} \\ &= 5.31 > 2.25 \end{aligned}$$

Because $F_y/F_e > 2.25$, the critical stress is determined as:

$$\begin{aligned} F_{cr} &= 0.877 F_e \\ &= 0.877(9.42 \text{ ksi}) \\ &= 8.26 \text{ ksi} \end{aligned} \tag{2}$$

Classify the flange for local buckling.

$$\lambda_{rf} = 0.56\sqrt{\frac{E}{F_y}} \tag{5b}$$
$$= 0.56\sqrt{\frac{(29{,}000 \text{ ksi})}{(50 \text{ ksi})}}$$
$$= 13.5$$

$$\lambda_f = \frac{b_f}{2t_f} \tag{5c}$$
$$= 7.06 < \lambda_{rf}$$

Thus, the flanges are nonslender, and $b_e = b_f/2$.

Classify the web for local buckling.

$$\lambda_{rw} = 1.49\sqrt{\frac{E}{F_y}} \tag{6b}$$
$$= 1.49\sqrt{\frac{(29{,}000 \text{ ksi})}{(50 \text{ ksi})}}$$
$$= 35.9$$

$$\lambda_w = \frac{h}{t_w} \tag{6c}$$
$$= 53.5 > \lambda_{rw}$$

Thus, the web is slender for axial compression.

To calculate the effective width, h_e, using Equation 6a, first determine the relationship between λ_w and $\lambda_{rw}\sqrt{\frac{F_y}{F_{cr}}}$.

$$\lambda_{rw}\sqrt{\frac{F_y}{F_{cr}}} = (35.9)\sqrt{\frac{(50 \text{ ksi})}{(8.26 \text{ ksi})}} \tag{6}$$
$$= 88.3 > \lambda_w = 53.5$$

Thus, the critical stress is low enough that no reduction is necessary.

$$h_e = h \tag{6a}$$

$$A_e = A_g \qquad \text{(from Eq. 4)}$$

Compute the axial compressive strength, P_n, using Equation 1.

$$P_n = F_{cr}A_e \tag{1}$$
$$= F_{cr}A_g$$
$$= (8.26 \text{ ksi})(10.3 \text{ in.}^2)$$
$$= 85.1 \text{ kips}$$

The nominal strengths of the other modes of buckling assuming no bracing provided by the decking system are presented in Table 1, where P_{nx}, P_{ny}, P_{nz}, and P_{nca} are the computed strengths for the major-axis flexural, minor-axis flexural, torsional, and

Table 1. Axial Strength for Various Buckling Modes	
Buckling Mode	**Axial Strength**
Major-axis flexural buckling	P_{nx} = 408 kips
Minor-axis flexural buckling	P_{ny} = 46.4 kips
Torsional buckling	P_{nz} = 165 kips
Constrained-axis torsional buckling	P_{nca} = 85.1 kips

constrained-axis torsional buckling modes, respectively. A comparison of the buckling capacities provides some interesting insights into the behavior. The minor-axis flexural buckling strength is significantly smaller than the torsional buckling strength because the unbraced length is the same for these two modes. Torsional buckling will always yield a larger strength than minor-axis flexural buckling for wide-flange members of the same unbraced length. The table also demonstrates the significant reduction in the strength for the constrained-axis torsional buckling mode versus the torsional buckling mode, which will always be the case when the location of bracing is offset along the minor-axis of the section. These values vary with the unbraced length as shown in Figure 3.

Bracing Requirement Checks

For the configuration described previously, determine if the decking system is adequate to brace the beam against constrained-axis torsional buckling at a required axial load of P_u = 250 kips.

To determine if the decking system is adequate to brace the beam, both stiffness and strength checks are necessary. First, the required stiffness is calculated, followed by an evaluation of the available stiffness. The required strength is then calculated (including a reduction based on the ratio of required stiffness to provided stiffness) and finally the available strength.

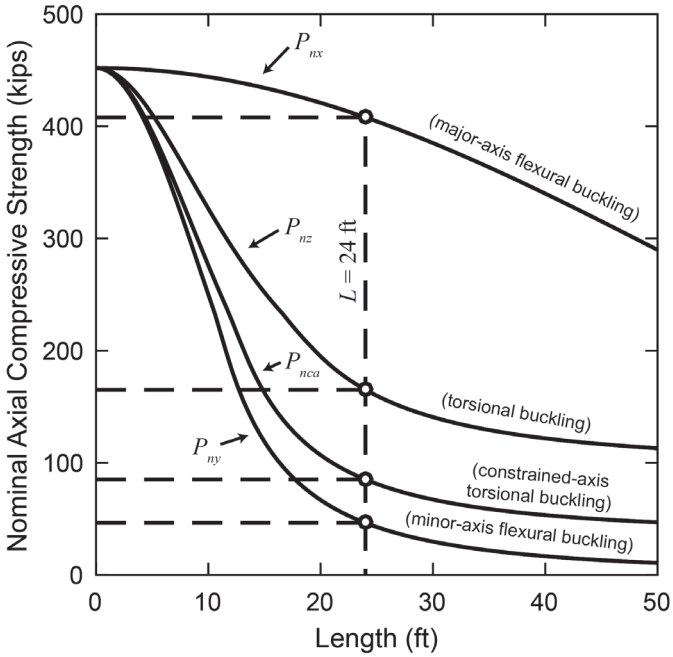

Fig. 3. Variation of axial strength with length.

Required Brace Stiffness

Recall that the value of x is the ratio of the effective area to the gross area at a critical stress equal to the required strength divided by the effective area. The x value needs to be determined iteratively. For this case, $x = 0.985$, as confirmed in the following calculations. A trial critical stress, F_{cr}, is calculated according to the definition of x given in Equation 8b.

$$A_e = xA_g \quad \text{(from Eq. 8b)}$$
$$= (0.985)(10.3 \text{ in.}^2)$$
$$= 10.1 \text{ in.}^2$$

$$F_{cr} = \frac{P_u}{A_e}$$
$$= \frac{(250 \text{ kips})}{(10.1 \text{ in.}^2)}$$
$$= 24.8 \text{ ksi}$$

As demonstrated in the baseline calculations, the flanges are nonslender ($b_e = b_f/2$) and the web is slender. Calculate the effective width, h_e, using Equation 6.

$$\lambda_{rw}\sqrt{\frac{F_y}{F_{cr}}} = (35.9)\sqrt{\frac{(50 \text{ ksi})}{(24.8 \text{ ksi})}}$$
$$= 51.0 < \lambda_w$$
$$h_e = \left(1 - 0.24\frac{\lambda_{rw}}{\lambda_w}\sqrt{\frac{F_y}{F_{cr}}}\right)1.31\frac{\lambda_{rw}}{\lambda_w}\sqrt{\frac{F_y}{F_{cr}}}h \quad \text{(6a)}$$
$$= \left(1 - 0.24\frac{(35.9)}{(53.5)}\sqrt{\frac{(50 \text{ ksi})}{(24.6 \text{ ksi})}}\right)1.31\frac{(35.9)}{(53.5)}\sqrt{\frac{(50 \text{ ksi})}{(24.6 \text{ ksi})}}(16.1 \text{ in.})$$
$$= 15.5 \text{ in.}$$

Compute the effective area, A_e, using Equation 4.

$$A_e = A_g - (h - h_e)t_w \quad (4)$$
$$= (10.3 \text{ in.}^2) - \left[(16.1 \text{ in.}) - (15.5 \text{ in.})\right](0.300 \text{ in.})$$
$$= 10.1 \text{ in.}^2$$

Compute the value x using Equation 8b.

$$x = \frac{A_e}{A_g} \quad (8b)$$
$$= \frac{(10.1 \text{ in.}^2)}{(10.3 \text{ in.}^2)}$$
$$= 0.981$$

The result is within the rounding error of the trial value; thus, $x = 0.985$ is confirmed.

Compute the stiffness reduction factor, τ, using Equation 8a.

$$P_y = A_g F_y$$
$$= (10.3 \text{ in.}^2)(50 \text{ ksi})$$
$$= 515 \text{ kips}$$

$$\frac{P_u}{xP_y} = \frac{(250 \text{ kips})}{(0.985)(515 \text{ kips})}$$
$$= 0.493 > 0.39$$

Because $\frac{P_u}{xP_y} > 0.39$, τ is calculated as:

$$\tau = -2.724\left(\frac{P_u}{P_y}\right)\ln\left(\frac{P_u}{xP_y}\right) \quad (8a)$$
$$= -2.724\left[\frac{(250 \text{ kips})}{(515 \text{ kips})}\right]\ln\left[\frac{(250 \text{ kips})}{(0.985)(515 \text{ kips})}\right]$$
$$= 0.936$$

Compute P_{ny}^*, using Equation 7c.

$$P_{ny}^* = 0.877\tau\frac{\pi^2 EI_y}{L^2} \quad (7c)$$
$$= 0.877(0.936)\frac{\pi^2(29{,}000 \text{ ksi})(15.3 \text{ in.}^4)}{(288 \text{ in.})^2}$$
$$= 43.3 \text{ kips}$$

The value P_{ny}^* represents the minor-axis flexural buckling strength considering the full length of the beam and with the level of inelasticity expected at the required axial strength. The value varies as shown in Figure 4.

Compute the required total brace stiffness, β_T, using Equation 10.

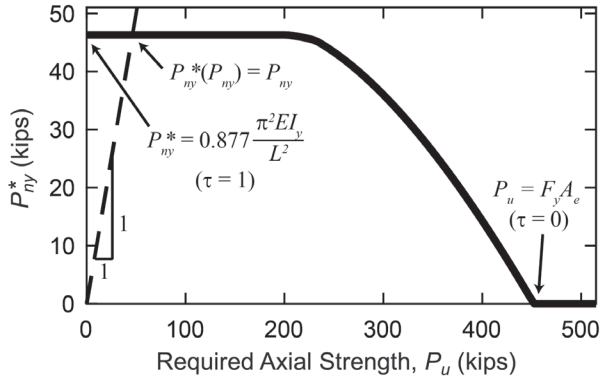

Fig. 4. Variation of P_{ny}^* *with required axial strength.*

$$\beta_T = \frac{1.5}{\phi}\frac{\left(P_u r_o^2 - P_{ny}^* h_o^2/2\right)^2}{\tau E I_y h_o^2} \tag{10}$$

$$= \frac{1.5}{(0.75)}\frac{\left[(250\text{ kips})(126\text{ in.}^2) - (43.3\text{ kips})(17.3\text{ in.})^2/2\right]^2}{(0.936)(29{,}000\text{ ksi})(15.3\text{ in.}^4)(17.3\text{ in.})^2}$$

$$= 10.1\text{ kip-in./rad/in.}$$

Compute the distortional stiffness of the beam web, β_{sec}, using Equation 11.

$$\beta_{sec} = \frac{3.3Et_w^3}{12h_0} = \frac{3.3(29{,}000\text{ ksi})(0.300\text{ in.})^3}{12(17.3\text{ in.})} \tag{11}$$

$$= 12.5\text{ kip-in./rad/in.}$$

Compute the required stiffness of the decking system, β_{Tb}, using Equation 12.

$$\beta_{Tb} = \frac{\beta_T}{\left(1 - \frac{\beta_T}{\beta_{sec}}\right)} \tag{12}$$

$$= \frac{(10.1\text{ kip-in./rad/in.})}{\left[1 - \frac{(10.1\text{ kip-in./rad/in.})}{(12.5\text{ kip-in./rad/in.})}\right]}$$

$$= 52.6\text{ kip-in./rad/in.}$$

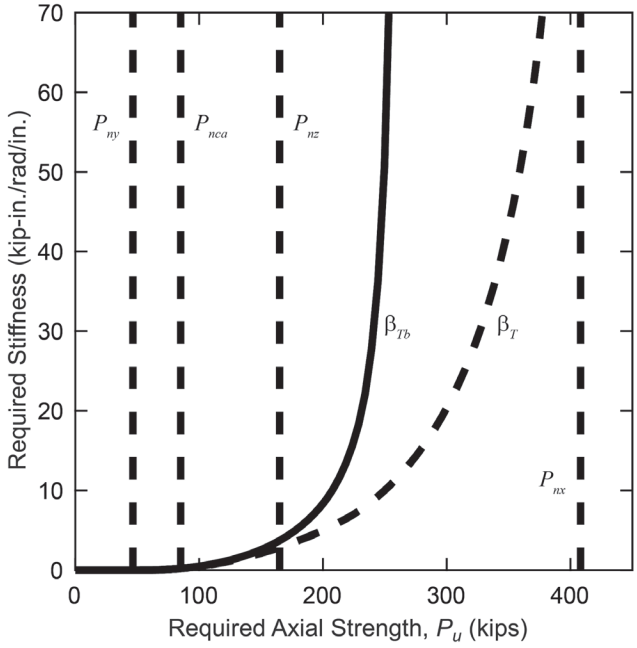

Fig. 5. Variation of required torsional bracing.

The required stiffness of the decking system varies with the required axial strength as shown in Figure 5. As can be seen for this case, the required stiffness is zero (or near zero due to simplifications in the derivation of the stiffness requirement) at the constrained-axis torsional buckling strength. It is a fairly modest value at the torsional buckling strength. The required stiffness of the decking system increases asymptotically to infinity for a required axial strength less than the major-axis flexural buckling strength, indicating that the distortional stiffness of the web is insufficient to make major-axis buckling the controlling mode of failure. Although it would be possible to reduce or eliminate cross-sectional distortion by providing transverse web stiffeners or struts between the decking system and bottom flange at a few locations along the length of the beam, the fabrication costs are likely to make such detailing impractical. Selecting a beam with a stockier web would be more prudent. It should be noted that the W18×35 has a web slenderness of 53.5 and is among the most slender rolled W-shaped sections. Sections with stockier webs will have fewer issues with cross-sectional distortion.

Available Brace Stiffness

To determine the available stiffness, the decking system is assumed to act in single curvature on each side of the span, as shown in Figure 6, and the adjacent beams are assumed to have similar demands on the decking system as the example beam. Thus, the stiffness contribution from each side is $2EI/L$, where EI is the flexural rigidity of the decking system and L is the deck span (Figure 7). Rigid connections are assumed between the beam and decking system.

On one side of the beam (left side in Figure 6), the concrete is in tension, and thus only the moment of inertia of the composite steel deck is conservatively relied upon. The moment of inertia of 20-ga. composite steel deck with a 3-in. depth is 0.920 in.^{4}/ft (Sputo, 2014). On the other side of the beam (right side in Figure 6), the concrete is in compression, and the moment of inertia of the composite slab is considered. The design moment of inertia of a 6-in. total depth composite slab constructed with 20-ga. composite steel deck with a 3-in. depth and normal weight concrete is 13.34 in.^{4}/ft (Sputo, 2014). Perimeter beams or those adjacent to an opening should only consider the stiffness of the side where the decking system is present.

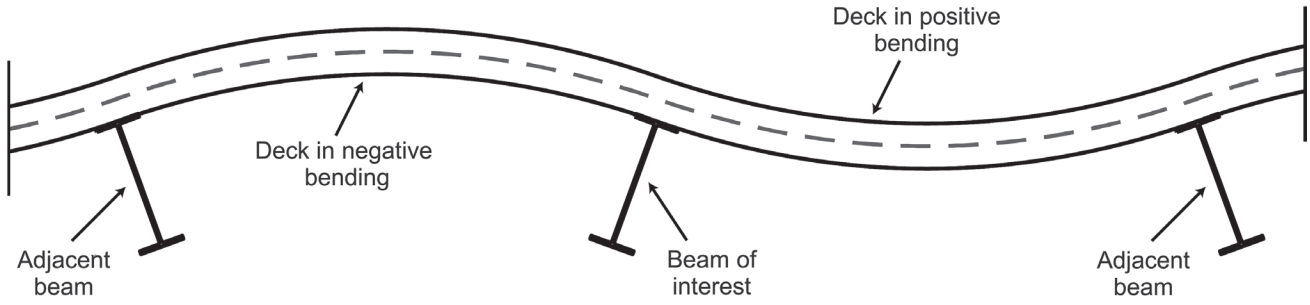

Fig. 6. Assumed deck bending mode.

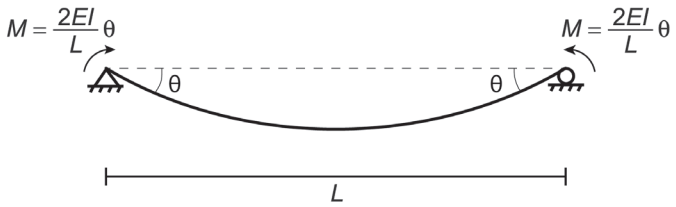

Fig. 7. Deck bending stiffness model.

Calculate the stiffness provided by the decking system, $\beta_{prov\text{-}b}$, as the sum of the contributions from both sides.

$$\beta_{prov-b} = \left(\frac{2EI}{L}\right)_{\text{left}} + \left(\frac{2EI}{L}\right)_{\text{right}}$$

$$= \frac{2(29{,}000 \text{ ksi})(0.920 \text{ in.}^4/\text{ft})\ 1 \text{ ft}/12 \text{ in.}}{(10 \text{ ft})(12 \text{ in.}/1 \text{ ft})} + \frac{2(29{,}000 \text{ ksi})(13.34 \text{ in.}^4/\text{ft})(1 \text{ ft}/12 \text{ in.})}{(10 \text{ ft})(12 \text{ in.}/1 \text{ ft})}$$

$$= 574 \text{ kip-in./rad/in.}$$

Because the stiffness provided by the decking system ($\beta_{prov\text{-}b}$ = 574 kip-in./rad/in.) is greater than the required stiffness of the decking system (β_{Tb} = 52.6 kip-in./rad/in.), the decking system has sufficient stiffness to brace the beam against constrained-axis torsional buckling at the required axial strength.

Required Brace Strength

The required brace strength is determined in accordance with Equation 15, which includes a reduction for surplus provided stiffness. Although the available stiffness of the decking system is substantially larger than the required stiffness, the effects of distortion need to be considered using Equation 16 to determine the provided total brace stiffness, β_{prov}.

$$\beta_{prov} = \left(\frac{1}{\beta_{prov-b}} + \frac{1}{\beta_{sec}}\right)^{-1} \quad \text{(from Eq. 16)}$$

$$= \left[\frac{1}{(574 \text{ kip-in./rad/in.})} + \frac{1}{(12.5 \text{ kip-in./rad/in.})}\right]^{-1}$$

$$= 12.2 \text{ kip-in./rad/in.}$$

This calculation demonstrates that cross-sectional distortion associated with web flexibility dominates the stiffness of this bracing system.

Compute the initial twist imperfection, θ_o, using Equation 14.

$$\theta_0 = \frac{L}{500h_o} \quad (14)$$

$$= \frac{(288 \text{ in.})}{500(17.3 \text{ in.})}$$

$$= 0.033 \text{ rad}$$

Compute the required brace strength, M_{br}, using Equation 15.

$$M_{br} = \frac{\beta_T \theta_o}{(2 - \beta_T/\beta_{prov})} \quad (15)$$

$$= \frac{(10.1 \text{ kip-in./rad/in.})(0.033 \text{ rad})}{\left[2 - (10.1 \text{ kip-in./rad/in.})/(12.2 \text{ kip-in./rad/in.})\right]}$$

$$= 0.287 \text{ kip-in./in.}$$

Available Brace Strength

The calculation of the available strength will vary depending on the specific situation, but will generally include assessment of the strength of the decking system, the strength of the connection between the decking system and beam, and the strength of the beam web.

Deck Bending Strength

On one side of the beam (left side in Figure 6), the decking system is in negative bending, the concrete is assumed to be cracked, and thus only the strength of the bare composite steel deck remains. The design strength of 20-ga. deck that is 3 in. deep is $\phi M_{n,neg}$ = 1.72 kip-in./in. (Sputo, 2014). On the other side of the beam (right side in Figure 6), the decking system is in positive bending, and the composite slab can be relied upon. The design strength of 20-ga. composite steel deck that is 3 in. deep and supporting 6-in. total depth normal weight concrete is $\phi M_{n,pos}$ = 5.10 kip-in./in. (Sputo, 2014). These strengths are parallel and additive; thus, the strength of the decking system is calculated as:

$$\begin{aligned}\phi M_n &= \phi M_{n,neg} + \phi M_{n,pos} \\ &= (1.72 \text{ kip-in./in.}) + (5.10 \text{ kip-in./in.}) \\ &= 6.82 \text{ kip-in./in.}\end{aligned}$$

Connection Strength

The connection between the decking system and the beam is provided by bearing and through the steel headed stud anchor. The interface between steel beams and composite slab has been studied extensively in the past, but predominantly under shear loading. Little guidance is available in the literature for the calculation of the twisting moment strength of the connection. For the purposes of this work, the moment is assumed to be taken by a force couple formed through tension in each steel headed stud anchor and compression on the beam flange as shown in Figure 8(a). The moment strength per unit length along the beam is then computed as the product of the strength of the controlling limit state of the force couple and the lever arm [taken as $b_f/3$ for the triangular stress distribution shown in Figure 8(a)] divided by the stud spacing. The strength of the force couple is computed from the limit states of steel headed stud tensile rupture, concrete pullout, concrete breakout, concrete crushing, and beam flange yielding.

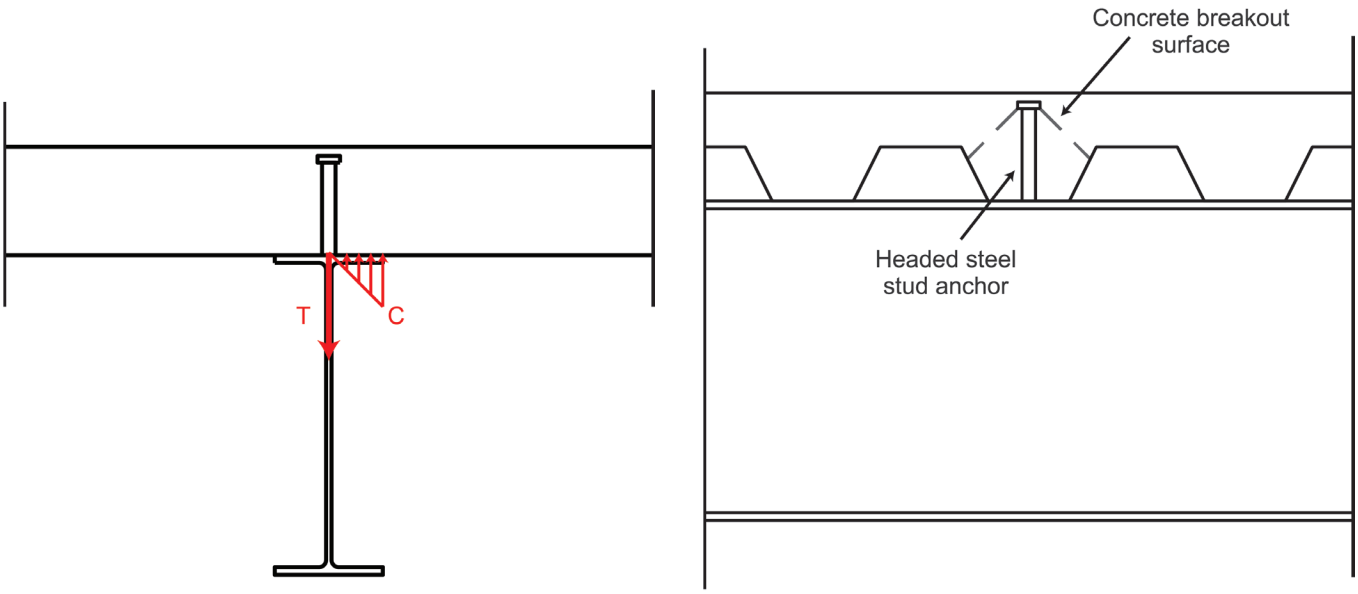

(a) Beam cross-section view *(b) Beam side view*

Fig. 8. Beam-to-deck connection.

Steel Tensile Strength

The strength of the steel headed stud anchor in tension is computed using the provisions of AISC *Specification* Section I8.3b (2016). The diameter of the shank of the steel headed stud anchor is 0.75 in. and the ultimate strength, F_u, is 65 ksi.

$$\begin{aligned}\phi R_n &= \phi F_u A_s \\ &= (0.75)(65 \text{ ksi})\frac{\pi}{4}(0.75 \text{ in.})^2 \\ &= 21.5 \text{ kips}\end{aligned}$$

Concrete Pullout Strength

Pullout of the headed stud anchor is determined using the provisions of ACI 318, Section 17.4.3 (ACI, 2014). For a ¾-in.-diameter steel headed stud anchor, the diameter of the head is 1.25 in.

Compute the bearing area, A_{brg}, as

$$\begin{aligned}A_{brg} &= \frac{\pi}{4}d_{head}^2 - \frac{\pi}{4}d_{shank}^2 \\ &= \frac{\pi}{4}(1.25 \text{ in.})^2 - \frac{\pi}{4}(0.75 \text{ in.})^2 \\ &= 0.785 \text{ in.}^2\end{aligned}$$

Compute the pullout strength as

$$\begin{aligned}\phi R_n &= \phi 8 A_{brg} f_c' \\ &= (0.70)8(0.785 \text{ in.}^2)(3 \text{ ksi}) \\ &= 13.2 \text{ kips}\end{aligned}$$

Concrete Breakout Strength

Hawkins and Mitchell (1984) derived an equation for the breakout strength of steel headed stud anchors embedded in a composite slab with composite steel deck based on the height of the stud, H_s, and rib width at mid-height of the composite steel deck, w_r. The height of the stud is taken as the total depth of the composite slab (6 in.) minus the required cover (0.5 in.) minus the height of the head of the stud (0.375 in.). Thus, the height of the stud, H_s, is taken as 5.125 in. The rib width at mid-height of the composite steel deck, w_r. is taken as 6 in.

$$\begin{aligned}A_c &= 2\sqrt{2}H_s w_r \\ &= 2\sqrt{2}(5.125 \text{ in.})(6.0 \text{ in.}) \\ &= 87.0 \text{ in.}^2 \\ \phi R_n &= \phi 4\sqrt{f_c'}A_c \\ &= (0.75)4\sqrt{3{,}000 \text{ psi}}(87.0 \text{ in.}^2) \\ &= 14{,}300 \text{ lb}\left(\frac{1 \text{ kip}}{1{,}000 \text{ lb}}\right) \\ &= 14.3 \text{ kips}\end{aligned}$$

As an alternative approach, Lawson and Hicks (2011) recommend taking the tensile strength of a headed stud anchor as 85% of its shear strength. This method yields results in strengths somewhat higher than by evaluating each limit state individually.

Concrete Crushing Strength

The bearing strength of the concrete is computed using the provisions of AISC *Specification* Section J8 (AISC, 2016).

Compute the bearing area, A_1, as the product of deck rib width (4.5 in.) and half the beam flange width [Figure 8(a)].

$$A_1 = (4.5 \text{ in.})(b_f/2)$$
$$= (4.5 \text{ in.})(6.00 \text{ in.}/2)$$
$$= 13.5 \text{ in.}^2$$

Compute the bearing strength as

$$\phi P_P = \phi 0.85 f_c' A_1$$
$$= (0.65)(0.85)(3 \text{ ksi})(13.5 \text{ in.}^2)$$
$$= 22.4 \text{ kips}$$

Beam Flange Bending Strength

The strength of the beam flange in bending is computed based on the plastic moment strength of a length of the flange equal to the stud spacing at a distance k_1 from the beam centerline and assuming the compressive couple force acts at a distance $b_f/3$ from the beam centerline.

$$\phi M_{n,flange} = \phi F_y \frac{t_f^2 s}{4}$$
$$= (0.90)(50 \text{ ksi})\frac{(0.425 \text{ in.})^2 (12 \text{ in.})}{4}$$
$$= 24.4 \text{ kip-in.}$$
$$\phi R_n = \frac{\phi M_{n,flange}}{(b_f/3 - k_1)}$$
$$= \frac{(24.4 \text{ kip-in.})}{\left[(6.00 \text{ in}/3) - (0.75 \text{ in.})\right]}$$
$$= 19.5 \text{ kips}$$

From the preceding calculations, the controlling limit state for the force within the couple is concrete pullout of the steel headed stud anchor. Combining that result with the lever arm of the couple and the spacing of the steel headed stud anchors, the controlling connection strength is calculated as:

$$\phi M_n = \frac{\phi R_n}{s}\left(\frac{b_f}{3}\right)$$
$$= \frac{(13.2 \text{ kips})}{(12 \text{ in.})}\left(\frac{6.00 \text{ in.}}{3}\right)$$
$$= 2.20 \text{ kip-in./in.}$$

Beam Web Bending Strength

It is expected that the out-of-plane bending demand on the beam web is less than the required strength of the connection; however, it is unclear how much less. For these calculations, the bending demand of the web is conservatively taken as the required brace strength. The strength of the beam web bending out of plane is computed as the plastic moment strength:

$$\phi M_n = \phi F_y \frac{t_w^2}{4}$$
$$= (0.90)(50 \text{ ksi})\frac{(0.300 \text{ in.})^2}{4}$$
$$= 1.01 \text{ kip-in./in.}$$

Table 2. Parametric Study Properties		
Property	**Case A**	**Case B**
Decking system stiffness, $\beta_{prov\text{-}b}$ (kip-in./rad/in.)	400	30
Decking system strength, ϕM_n (kip-in./in.)	5	1
Connection force couple strength, ϕR_n (kips)	10	0.4

Given that the strength of the beam web (ϕM_n = 1.01 kip-in./in.) is less than that of either the decking system or the connection, it is the controlling strength of the brace. Further, this strength is sufficient because it exceeds the required brace strength (M_{br} = 0.287 kip-in./in.).

Example Summary

Having met both the stiffness and strength requirements, the decking system is adequate to brace the beam against constrained-axis torsional buckling at the required axial strength.

The calculations presented in this example are not intended to cover every possible situation. Engineering judgment is necessary —especially when computing available braced stiffness and strength—to ensure that rational and reliable load paths exist and that all relevant sources of flexibility have been accounted for. Cases such as perimeter beams, where a decking system is present on only one side of the member, or bare composite steel or roof deck with a wide bottom flat, where the connection between the decking system and beam may be flexible, should be approached with special care.

Parametric Study

The calculations to check the bracing requirements, such as presented in the example, are quite involved and are generally impractical for typical designs. Noting that, in this section, a parametric study is presented with two goals: (1) to identify conditions that are most beneficial for relying upon the rotational bracing provided by the decking system and (2) to develop rules of thumb such that in specific typical cases, the bracing provided by the decking system can be taken advantage of without the need to perform full calculations.

Of interest in this study is the calculation of the axial strength of the beam for a given decking system configuration. The relevant parameters of the decking system configuration are the provided stiffness, $\beta_{prov\text{-}b}$, and the moment strength, ϕM_n (noting that the decking system, connection, or beam web may control strength). The two requirements can be stated as Equations 17 and 18.

$$\beta_{prov} \geq \beta_T \tag{17}$$

$$\phi M_n \geq M_{br} \tag{18}$$

Alternatively, noting the relationship between β_T and M_{br} in Equation 15, the requirements can be combined as in Equations 19 and 20, where the moment requirement has been converted into a stiffness requirement.

$$\beta_{limit} \geq \beta_T \tag{19}$$

$$\beta_{limit} = \min\left(\beta_{prov}, \frac{2\phi M_n}{\theta_o + \phi M_n / \beta_{prov}}\right) \tag{20}$$

The axial strength is calculated iteratively, not directly, as the maximum axial load for which the beam can be considered braced against constrained-axis torsional buckling (i.e., satisfying Equation 19). This axial load, termed $P_{u,braced}$, is analogous to the design constrained-axis torsional buckling strength and comparable to design strengths for other buckling modes.

For the parametric study, two generic bracing cases are defined. The first case, Case A, is representative of a composite slab similar to what was computed in the example presented in the previous section. The three defining factors are the decking system stiffness, $\beta_{prov\text{-}b}$, the decking system strength, ϕM_n, and the connection force couple strength, ϕR_n. Each of these values, given in Table 2, is marginally lower than what was calculated in the example so as to broaden the range of applicability. The second case, Case B, is representative of a steel roof deck (with ribs perpendicular to the beam). The strengths and stiffnesses are accordingly lower than that of the composite slab, including for the connection force couple strength which is controlled, for example, by the uplift strength of a spot weld.

The variation of $P_{u,braced}$ with length for a W18×35 beam is shown in Figure 9. The results in the figure show the two different cases (Table 2), an additional case of β_{limit} = 0, and the constrained-axis torsional buckling design strength computed without accounting for any bracing. It is expected,

logically, that for $\beta_{limit} = 0$, the maximum permitted axial load will equal the constrained-axis torsional buckling strength from the code equations (i.e., $P_{u,braced} = \phi P_{nca}$). However, as can be seen in Figure 9, the two values differ. The differences are due to simplifications made in the derivation of the brace stiffness requirements and the fact that the derivation was not intended to be applicable for zero brace stiffness. It is expected that for practical values of β_{limit}, the method is accurate.

The parametric study was performed by computing $P_{u,braced}$ for each wide flange shape in the AISC Shapes Database (AISC, 2017b) with a weight less than or equal to 150 lb/ft, for both generic bracing configurations (Table 2) and for a range of lengths from $L/d = 5$ to $L/d = 50$, where d is the section depth. The results of the parametric study are presented in Figure 10. In each of the plots of Figure 10, the ratio of $P_{u,braced}$ to a design strength is plotted as a function of the unbraced length of the beam. Each line represents one cross section. The lines are shaded based on the cross-section web slenderness, h/t_w. The plots on the left-hand side are for Case A, while the plots on the right hand side are for Case B.

In Figures 10(a) and 10(b), $P_{u,braced}$ is plotted with respect to the design constrained-axis torsional buckling strength. These plots show most directly the increase in calculated strength by accounting for the rotational stiffness of the decking system. With the greater stiffness and strength of Case A, the calculated strength increases by as much as a factor of 6. Whereas for Case B, the calculated strength increases by as much as a factor of 3, but in some cases decreases, indicating that steel roof deck is not effective in providing bracing against constrained-axis torsional buckling. For both cases, the largest increases are for cross sections with higher web slenderness.

In Figures 10(c) and 10(d), $P_{u,braced}$ is plotted with respect to the design torsional buckling strength. Again, the greater stiffness and strength of Case A are demonstrated in the higher strength ratios. A key result shown in Figure 10(c) is that for Case A and for all wide flange cross sections weighing 150 lb/ft or less, the constrained-axis torsional buckling strength is nearly or at least equal to the calculated torsional buckling strength [the ratio $P_{u,braced}$ to ϕP_{nx} has a minimum value of 0.975 in Figure 10(c)]. For comparison, the ratio ϕP_{nca} to ϕP_{nz} has a minimum value of 0.371 over the same range (Figure 11). The lowest values in that ratio occur for cross sections with lower web slenderness.

In Figures 10(e) and 10(f), $P_{u,braced}$ is plotted with respect to the design major-axis flexural buckling strength. The second key result is shown in Figure 10(e). For Case A and for all wide flange cross sections weighing 150 lb/ft or less, the constrained-axis torsional buckling strength is at least half of the calculated major-axis flexural buckling strength [the ratio $P_{u,braced}$ to ϕP_{nx} has a minimum value of 0.577 in Figure 10(e)]. For comparison, the ratio ϕP_{nca} to ϕP_{nx} has a minimum value of 0.129 over the same range (Figure 12). The lowest values in that ratio occur for cross sections with higher web slenderness.

For the cases examined, the key results from Figure 10 are that the constrained-axis torsional buckling strength is nearly equal to or greater than either the torsional buckling strength or half the major-axis flexural buckling strength; these are potentially useful rules of thumb. These results can be conservatively used for cases within the range of the study—namely, wide flange shapes weighing 150 lb/ft or less, decking system properties meeting or exceeding those listed in Table 2 for Case A, and span lengths between 5 and 50 times the beam depth.

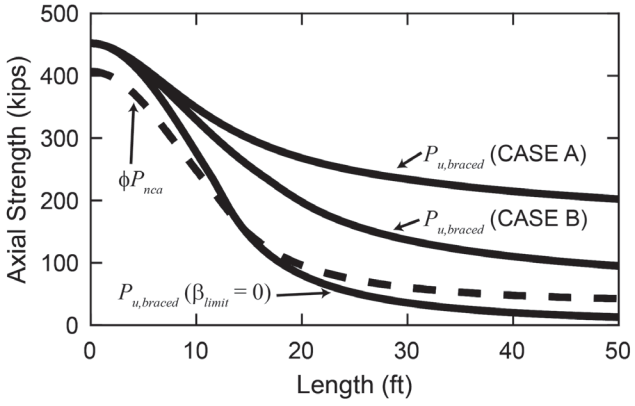

Fig. 9. Variation of axial strength with length.

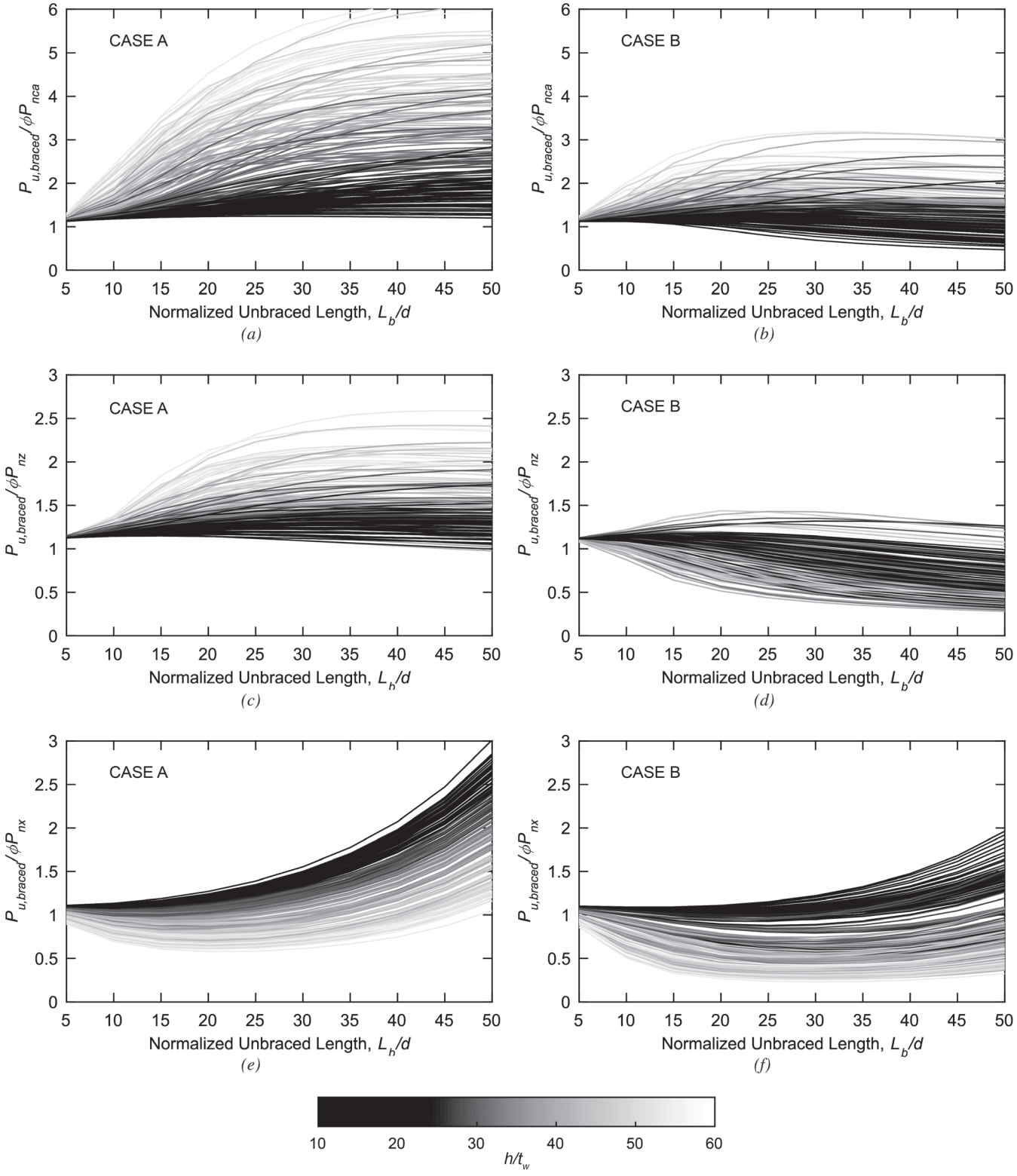

Fig. 10. Parametric study results.

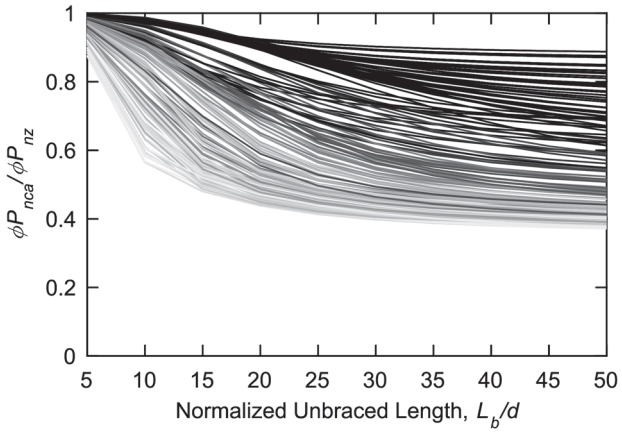

Fig. 11. Comparison of axial strength, P_{nca} *to* P_{nz}.

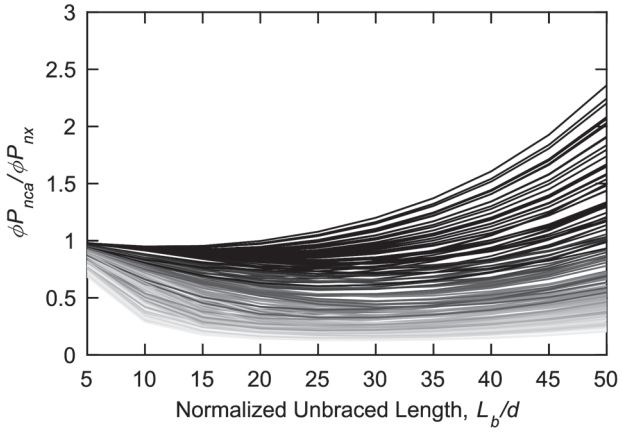

Fig. 12. Comparison of axial strength, P_{nca} *to* P_{nx}.

CONCLUSIONS

Accounting only for the lateral restraint provided by steel roof deck or composite floor deck may lead to a situation where the computed axial strength of a beam is controlled by constrained-axis torsional buckling. The stiffness and strength requirements developed in this paper allow for the inclusion of the rotational restraint provided by steel roof deck or composite floor deck. The inclusion of this restraint can lead to a significant increase in the calculated axial strength. The requirements are based on the results of prior studies, and an example was presented to illustrate their use. A parametric study was performed to identify cases when accounting for the rotational restraint was most beneficial and to develop rules of thumb, with the key result being that for wide-flange beams that weigh 150 lb/ft or less, the rotational restraint provided by typical composite deck to interior beams is sufficient to achieve strengths of at least 50% of the major-axis flexural buckling strength.

SYMBOLS

A	Factor applied to ideal torsional brace stiffness to control deformations and brace moments
A_1	Loaded area of concrete, in.^{2}
A_{brg}	Bearing area, in.^{2}
A_c	Concrete breakout failure area, in.^{2}
A_e	Effective area, in.^{2}
A_g	Gross cross-sectional area, in.^{2}
A_s	Cross-sectional area of steel headed stud anchor, in.^{2}
E	Modulus of elasticity of steel = 29,000 ksi
EI	Flexural rigidity of the decking system, kip-in.^{2}
F_{cr}	Critical stress, ksi
F_e	Elastic buckling stress, ksi
F_y	Yield stress, ksi
F_u	Tensile strength, ksi
G	Shear modulus of steel = 11,200 ksi
H_s	Height of steel headed stud anchor, in.
I_x	Major-axis moment of inertia, in.^{4}
I_y	Minor-axis moment of inertia, in.^{4}
J	Torsional constant, in.^{4}
L	Beam or deck span, in.
L_{cz}	Effective torsional length, in.
M_{br}	Required brace strength, kip-in.
M_n	Nominal moment strength, kip-in.
$M_{n,flange}$	Nominal moment strength of flange, kip-in.
$M_{n,neg}$	Nominal negative moment strength of the decking system, kip-in.
$M_{n,pos}$	Nominal positive moment strength of the decking system, kip-in.
P_n	Nominal compressive strength, kips
P_{nca}	Nominal compressive strength for the limit state of constrained-axis torsional buckling, kips
P_{nx}	Nominal compressive strength for the limit state of major-axis flexural buckling, kips
P_{ny}	Nominal compressive strength for the limit state of minor-axis flexural buckling, kips
P_{ny}^*	Minor-axis flexural buckling strength with full column length, kips
P_{nz}	Nominal compressive strength for the limit state of torsional buckling, kips
P_p	Nominal bearing strength, kips
P_u	Required axial compressive strength, kips
$P_{u,braced}$	Maximum required axial compressive strength that can be considered braced, kips
P_y	Axial yield strength, kips
Q	Net reduction factor accounting for all slender compression elements
R_n	Nominal strength, kips
a	Distance from centroid to brace point, in.
b_f	Width of flange, in.
b_e	Reduced effective width of half-flange, in.
d	Depth of section, in.
d_{head}	Head diameter of steel headed stud anchor, in.
d_{shank}	Shank diameter of steel headed stud anchor, in.
f_c'	Specified compressive strength of concrete, ksi
h	Web height, in.
h_e	Reduced effective web height, in.
h_o	Distance between flange centroids, in.
k_1	Distance from web center line to flange toe of fillet, in.
n_b	Number of intermediate braces

r_o	Polar radius of gyration, in.
r_x	Major-axis radius of gyration, in.
r_y	Minor-axis radius of gyration, in.
s	Spacing of steel headed stud anchors, in.
t_f	Thickness of flange, in.
t_w	Thickness of web, in.
w_r	Rib width at mid-height of composite steel deck, in.
x	Ratio of the effective area to the gross area
β_{limit}	Limiting provided brace stiffness including consideration of brace strength
β_{prov}	Total provided brace stiffness
$\beta_{prov\text{-}b}$	Provided stiffness of the decking system
β_{sec}	Web distortional stiffness
β_T	Required brace stiffness
β_{Tb}	Required stiffness of the decking system
λ_f	Width-to-thickness ratio for flange
λ_{rf}	Limiting width-to-thickness ratio for flange
λ_w	Width-to-thickness ratio for web
λ_{rw}	Limiting width-to-thickness ratio for web
ϕ	Resistance factor
θ_0	Initial twist imperfection
τ	Stiffness reduction factor
ω	Finite brace stiffness factor = 0.90

REFERENCES

ACI (2014), *Building Code Requirements for Structural Concrete and Commentary*, ACI 318-14, American Concrete Institute, Farmington Hills, Mich.

AISC (2010), *Specification for Structural Steel Buildings*, ANSI/AISC 360-10, American Institute of Steel Construction, Chicago, Ill.

AISC (2016), *Specification for Structural Steel Buildings*, ANSI/AISC 360-16, American Institute of Steel Construction, Chicago, Ill.

AISC (2017a), *Steel Construction Manual*, American Institute of Steel Construction, Chicago, Ill.

AISC (2017b), *Shapes Database*, v15.0, American Institute of Steel Construction, Chicago, Ill.

AISC (2018), *Seismic Design Manual*, American Institute of Steel Construction, Chicago, Ill.

Errera, S.J., and Apparao, T.V.S.R. (1976), "Design of I-Shaped Columns with Diaphragm Bracing," *Journal of the Structural Division*, ASCE, Vol. 102, No. 9, pp. 1,685–1,701.

Hawkins, N., and Mitchell, D. (1984), "Seismic Response of Composite Shear Connections," *Journal of Structural Engineering*, ASCE, Vol. 110, No. 9, pp. 2,120–2,136.

Helwig, T., and Yura, J. (1999), "Torsional Bracing of Columns," *Journal of Structural Engineering*, Vol. 125, No. 5, pp. 547–555.

Kaehler, R.C., White, D.W., and Kim, Y.D. (2011), *Frame Design Using Web-Tapered Members*, Design Guide 25, American Institute of Steel Construction, Chicago, Ill.

Lawson, R.M., and Hicks, S.J. (2011), *Design of composite Beams with Web Openings*, SCI Publication P355, Steel Construction Institute, Berkshire, United Kingdom.

Liu, D., Davis, B., Arber, L., and Sabelli, R. (2013), "Torsional and Constrained-Axis Flexural-Torsional Buckling Tables for Steel W-Shapes in Compression," *Engineering Journal*, AISC, Vol. 50, No. 4, pp. 205–247.

Sputo, T. (2014), *Floor Deck Design Manual*, Steel Deck Institute, Glenshaw, Pa.

Timoshenko, S.P., and Gere, J.M. (1961), *Theory of Elastic Stability,* 2nd Ed., McGraw-Hill, New York, N.Y.